Sequential ^{1}H NMR Assignments and Secondary Structure of an IgG-Binding Domain from Protein G†

L.-Y. Lian,*,‡ J. C. Yang,‡ J. P. Derrick,§ M. J. Sutcliffe,‡ G. C. K. Roberts,‡,§ J. P. Murphy,∥ C. R. Goward,∥ and T. Atkinson∥

Biological NMR Centre and Department of Biochemistry, University of Leicester, University Road, Leicester LE1 7RH, U.K., and Division of Biotechnology, PHLS Centre for Applied Microbiology and Research, Porton Down, Salisbury, Wiltshire SP4 0JG, U.K.

Received February 26, 1991; Revised Manuscript Received April 9, 1991

ABSTRACT: Protein G is a member of a class of cell surface bacterial proteins from *Streptococcus* that bind IgG with high affinity. A fragment of molecular mass 6988, which retains IgG-binding activity, has been generated by proteolytic digestion and analyzed by ^{1}H NMR. Two-dimensional DQF-COSY, TOCSY, and NOESY spectra have been employed to assign the ^{1}H NMR spectrum of the peptide. Elements of regular secondary structure have been identified by using nuclear Overhauser enhancement, coupling constant, and amide proton exchange data. The secondary structure consists of a central α-helix (Ala28–Val44), flanked by two portions of β-sheet (Val5–Val26 and Asp45–Lys62). This is a fundamentally different arrangement of secondary structure from that of protein A, which is made up of three consecutive α-helices in free solution (Torigoe et al., 1990). We conclude that the molecular mechanisms underlying the association of protein A and protein G with IgG are different.

Proteins that bind to the constant region (Fc) of IgG are located on the surface of a variety of staphylococci and streptococci (Langone, 1982). The best known of these is protein A from *Staphylococcus aureus*, whose ability to bind IgG has been exploited in many immunochemical methods. Protein G is a cell-wall-associated binding protein from *Streptococcus* that has high affinity for IgG from a wide range of mammalian sources [reviewed by Björck and Åkerström (1990)]. Several groups have reported complete or partial DNA sequences for the gene for protein G from several strains of *Streptococcus* (Fahnestock et al., 1990; Guss et al., 1986; Olsson et al., 1987; Goward et al., 1990). The whole protein G molecule is approximately 600 amino acid residues in length; the regions responsible for IgG binding have been assigned to three similar stretches of amino acid sequence, 70 residues long, each of which folds into a separate domain (Goward et al., 1991). The first two domains are identical in sequence and the third domain differs from the first two by only four amino acid substitutions. A truncated form of protein G (protein G′), containing all three IgG-binding domains (M_r = 20000), has been expressed in *Escherichia coli* and purified: it retains high affinity for IgG (Goward et al., 1990). Single IgG-binding domains from protein G have also been expressed and isolated from *E. coli* and have been shown to retain IgG-binding capability (Guss et al., 1986; Fahnestock et al., 1990). These small polypeptides are therefore a useful starting point for an analysis of the structure and mechanism of binding of protein G to IgG.

Protein A from *S. aureus* also contains repeating IgG-binding domains, but these show no sequence homology with the IgG-binding domains from protein G. The three-dimensional structure of the IgG-binding domain of protein A complexed with Fc has been determined by X-ray crystallography (Deisenhofer, 1981). This shows contacts between two α-helices in protein A and residues in the C_H2 and C_H3 domains of Fc. A recent analysis of the free solution structure of the IgG-binding domain of protein A by ^{1}H nuclear magnetic resonance (NMR)[1] has demonstrated the presence of a third α-helix at the C terminus, which is postulated to be disrupted on formation of the complex with Fc (Torigoe et al., 1990). The observation that protein G binding to Fc is competitive with respect to protein A, and therefore binds to the same site on Fc, raises the possibility that the folding of both proteins is the same, despite their lack of sequence homology (Stone et al., 1989). To address this question, we have assigned the ^{1}H NMR spectrum of the IgG-binding domain of protein G and determined its secondary structure.

Experimental Procedures

Preparation and Purification of the IgG-Binding Domain. Truncated protein G (protein G′, which contains three IgG-binding domains) was expressed in *E. coli* and purified as described by Goward et al. (1990). Proteolytic digestion of this protein to obtain the individual IgG-binding domains was carried out in 20 mM Tris-HCl (pH 7.5) at 37 °C for 48 h, with protein G′ at 11 mg/mL and *S. aureus* V8 protease at 30 μg/mL. The digestion products were separated on a FPLC system (Pharmacia) using a Mono Q 10/10 column, equilibrated in 20 mM Tris-HCl (pH 7.5; buffer A). After the sample was loaded, the column was washed at 4 mL/min for 10 min with buffer A and then three separate peptides were eluted with a linear gradient over 20 min from buffer A to Buffer A plus 0.3 M NaCl (pH 7.5). The second fragment eluted at A plus 0.13 M NaCl and was selected for further study. It ran as a single band on an SDS–17% polyacrylamide

† This work was supported by the Science and Engineering Research Council and The Royal Society (M.J.S.).

‡ Biological NMR Centre, University of Leicester.
§ Department of Biochemistry, University of Leicester.
∥ PHLS Centre for Applied Microbiology and Research.

[1] Abbreviations: NMR, nuclear magnetic resonance; ELISA, enzyme-linked immunosorbent assay; DQF-COSY, two-dimensional double-quantum-filtered correlated spectroscopy; TOCSY, two-dimensional total correlation spectroscopy; NOE, nuclear Overhauser effect; NOESY, two-dimensional NOE spectroscopy.

0006-2960/91/0430-5335$02.50/0 © 1991 American Chemical Society

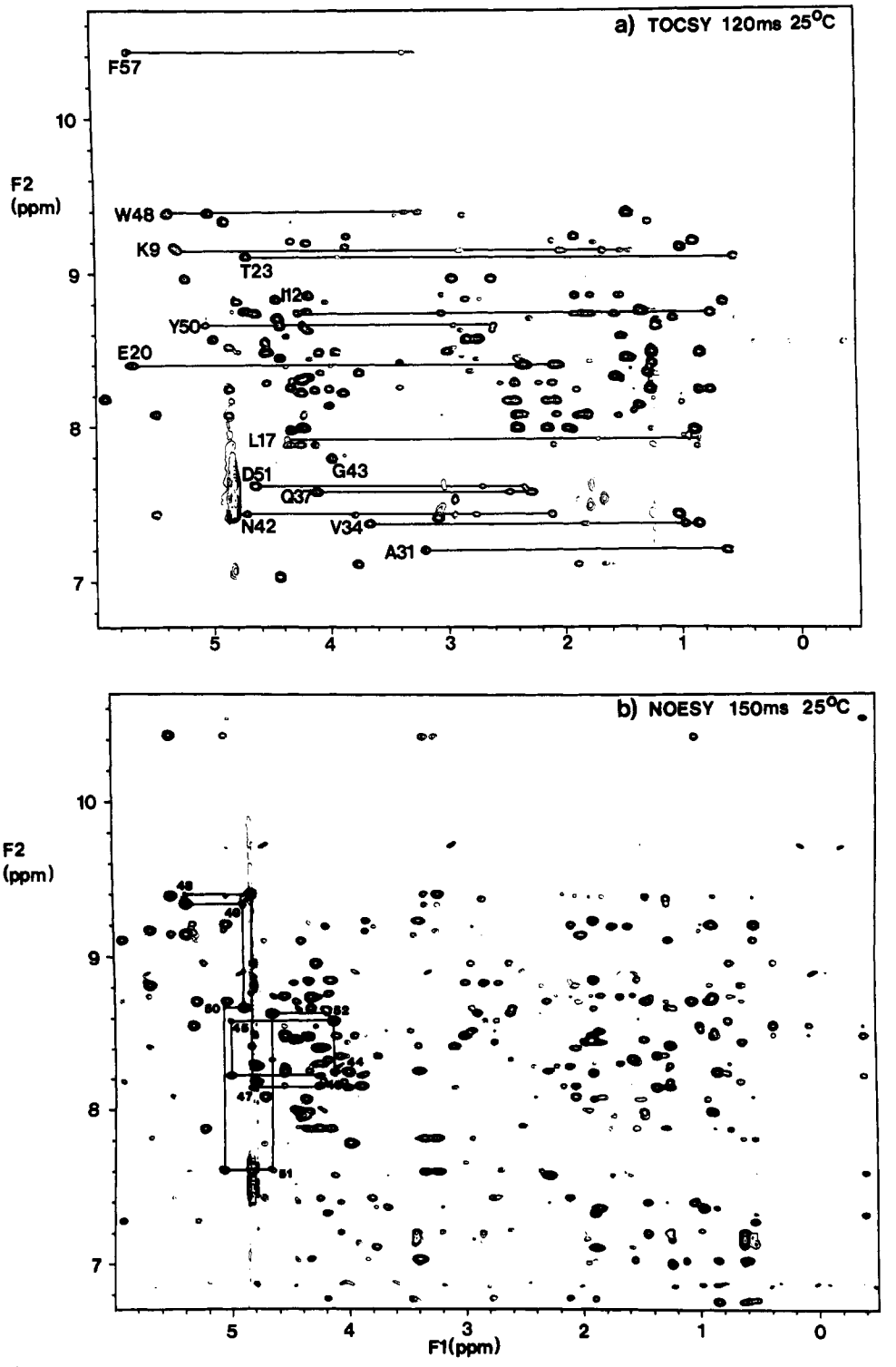

FIGURE 1: NH amide/aromatic (F_2 axis)–aliphatic (F_1 axis) region of the IgG-binding domain of protein G in 90%H_2O/10%D_2O at 25 °C, pH 4.2. (a) TOCSY spectrum (120-ms mixing time). Examples are shown of direct and relayed connectivities of the spin systems for selected residues. (b) NOESY spectrum (150-ms mixing time). A selected stretch of $C^{\alpha}H(i)$–NH(i) and $C^{\alpha}H(i)$–NH($i+1$) connectivities is shown, with the residue numbered at the $C^{\alpha}H(i)$–NH(i) cross-peak.

gel. N-Terminal sequence analysis gave the sequence LTPAVTTYKLVINGKTLKGETT. The C terminus of the fragment was unequivocally identified by molecular mass determination using electrospray mass spectrometry (calculated molecular mass for the sequence in Table I and Figure 3 = 6988, measured molecular mass = 6989). An ELISA procedure was used to confirm the IgG-binding activity of the polypeptide (Goward et al., 1990).

Samples for NMR spectroscopy were 1.5 mM solutions in either 90%H_2O/10%D_2O (pH 4.2 or 3.1, 100 mM sodium phosphate) or in 99.96% D_2O at the same pHs. Slowly exchanging amide protons were identified from the TOCSY spectrum recorded on a sample prepared by lyophilizing the protein from H_2O and redissolving it in D_2O immediately before use.

NMR Spectroscopy. NMR experiments were performed on Bruker AMX600 and AM500 spectrometers with ^1H resonance frequencies of 600.13 and 500.13 MHz, respectively. The NMR measurements were made at 25 and 37 °C. All spectra were recorded in the pure phase absorption mode according to the time-proportional phase incrementation method (Redfield & Kuntz, 1975; Marion & Wüthrich, 1983).

Chemical shifts were measured from dioxane and corrected by assigning the dioxane peak to 3.77 ppm from sodium 2,2-dimethyl-2-silapentane-5-sulfonate (DSS).

The proton 90° pulse widths employed were 12 μs (for the AMX600) and 8 μs (for the AM500). For the TOCSY experiments spin-locking fields of 8 kHz and either the MLEV-17 (Bax & Davis, 1985) or the DIPSI-II (Shaka et al., 1988) spin-locking sequence of total mixing times of 60 and 120 ms were used. NOESY data were collected with mixing times of 50, 100, 150, and 200 ms.

For measurements in water, neither the hard echo pulse (Sklenar & Bax, 1987; Lian, 1988) nor the 1-$\bar{1}$ pulse alone were able to suppress the water signal to a sufficiently low level to avoid radiation damping, due to the low concentration of the protein. An alternative method was used that combines a soft presaturation (63-db attenuation) and a 1-$\bar{1}$ pulse (L.-Y. Lian & J. C. Yang, unpublished results). In the NOESY experiment, a very soft presaturation pulse was applied during the preparation period and a 1-$\bar{1}$ pulse replaced the final single observation pulse. The pulse sequence used for the TOCSY experiment incorporated a similar water suppression method; a soft presaturation pulse was applied during the preparation, and after the spin-lock period, a three-pulse sequence was used that includes a flip-back 90° pulse as the read pulse. This technique is similar to a method suggested previously (Sklenar & Bax, 1987). Compared with a normal presaturation method, the quality of a 2D spectrum obtained in this way was significantly improved with removal of the "bleaching" in the fingerprint region of the spectrum. Furthermore, the baseline distortion is much lower when compared with a simple 1-$\bar{1}$ pulse. The receiver phase was optimised by using the "ADC" instead of the "GO" command for explicit acquisition, in both the NOESY and TOCSY experiments, to reduce baseline distortion (Marion & Bax, 1988).

Typical data set sizes were 512 increments of 2K data points. These yielded, after zero-filling, spectra with digital resolution of about 2–3 Hz/point in each dimension. For estimation of J-coupling constants, typical data set sizes were 2K by 1K; zero-filling gave spectra with digital resolution of about 0.8 Hz/point in each dimension. Prior to Fourier transformation, a Lorentzian-to-Gaussian window function was applied in both F_2 and F_1. Where necessary, base-plane distortion was corrected after 2D Fourier transformation.

Results and Discussion

Assignment of the ^1H NMR Spectrum of Protein G IgG-Binding Domain. The complete assignment of the ^1H NMR spectrum of the IgG-binding domain of protein G was achieved by using standard 2D homonuclear methods (Wüthrich, 1986; Basus, 1989). Initially, different types of amino acid residues were identified via through-bond connectivities (DQF-COSY and TOCSY), followed by the identification of sequential interresidue through-space connectivities (NOESY). Examples of the TOCSY and NOESY spectra are shown in Figures 1 and 2.

The DQF-COSY spectrum was required to identify the direct three-bond scalar connectivities, particularly in the fingerprint region. The success of this approach relies upon obtaining the maximal number of cross-peaks in the fingerprint region. In most cases, for experiments carried out in water, this is limited by the presaturation of the water signal, which leads to bleaching of $C^\alpha H$–NH cross-peaks arising from $C^\alpha H$ resonances that are degenerate with the water signal. However, by using the water suppression method described in the experimental section, it was possible to remove this bleaching

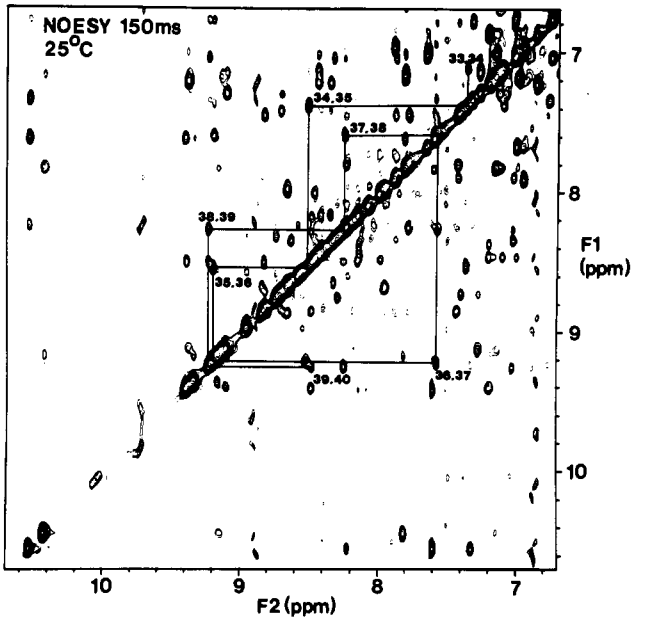

FIGURE 2: NH (F_1 axis)–NH (F_2 axis) of the 150-ms NOESY spectrum of the IgG-binding domain of protein G, measured under the same conditions as Figure 1. The NH(i)–NH(i + 1) sequential NOE connectivities for some residues are indicated, the first giving the residue number in F_1 and the second the residue number in F_2.

effect from TOCSY spectra. All except two of the expected $C^\alpha H$–NH cross-peaks were observed. The remaining two were identified by performing the experiment at a different temperature. Once all the fingerprint $C^\alpha H$–NH connectivities had been identified, TOCSY spectra at two mixing times (60 and 120 ms) were used to delineate almost all the spin systems by developing the spin system from the NH signal. It was possible to obtain TOCSY spectra at long mixing times without significant attenuation of the relayed cross-peak intensities because the small size of the protein gave rise to long transverse relaxation times. Of the 61 possible residues whose spin systems could in principle be traced from the amide resonance (64 residues minus N-terminal Leu and two Pro residues), complete spin systems were identified for 59 of the residues by using the TOCSY spectra obtained at mixing times of 60 and 120 ms. For the remaining residues, where complete delineation of spin systems from the amide protons was not feasible (due either to unfavorable intervening scalar coupling constants or to substantial attenuation of $C^\alpha H$–NH cross-peaks by NH exchange), the amide to side-chain proton connectivities were identified as far along the chain as possible and the identification of the spin system was completed by using the aliphatic part of the spectrum. Thus, while it was relatively easy to identify the complete spin system for the Val residues starting from the amide protons, the same was not true for the Leu and Ile residues, although it was possible to obtain relayed connectivities from the NH to the γ protons. To complete the spin-system identification, it was necessary to extract the information from the methyl region of the TOCSY and DQF-COSY spectra.

The $C^\beta H_2$ resonances of Asn and the $C^\gamma H_2$ resonances of Gln were identified from NOE connectivities with their respective side-chain amide protons. This method distinguished Asn from Asp and Gln from Glu side-chain resonances. The lysine residues were also easily identified by using TOCSY cross-peaks involving $C^\alpha H$–NH, $C^\beta H_2$, $C^\gamma H_2$, and in some cases $C^\delta H_2$ and $C^\epsilon H_2$; these cross-peaks were confirmed by matching a corresponding set from the side-chain $N^\epsilon H_3^+$ to $C^\epsilon H_2$, $C^\delta H_2$, and $C^\gamma H_2$ at pH 3.1. At higher pH values, under

Table I: ^{1}H NMR Chemical Shifts of the IgG-Binding Domain from Protein G at 25 °C and pH 4.2 (in ppm)[a]

residue	NH	C$^\alpha$H	C$^\beta$H	other	residue	NH	C$^\alpha$H	C$^\beta$H	other
Leu1[b]					Ala29	8.14	4.00	1.35	
Thr2	8.75	4.72	4.18	CγH$_3$ 1.33	Thr30	8.35	3.76	4.06	CγH$_3$ 1.28
Pro3		4.45	2.37, 1.97	CγH$_2$ 2.05, C$^\delta$H 3.95, 3.79	Ala31	7.19	3.19	0.61	
					Glu32	8.44	4.16	2.40	CγH$_2$ 2.75
Ala4	8.45	4.41	1.11		Lys33	7.11	3.82	1.88	CγH$_2$ 1.36, C$^\delta$H 1.65, 1.57, C$^\epsilon$H$_2$ 2.94
Val5	7.97	4.33	1.91	CγH$_3$ 0.87	Val34	7.36	3.66	1.83	CγH$_3$ 0.96, 0.85
Thr6	8.47	4.54	4.08	CγH$_3$ 0.83	Phe35	8.52	4.85	3.46, 2.92	C$^\delta$H$_2$ 6.60, C$^\epsilon$H$_2$ 6.77, CζH 6.66
Thr7	8.24	4.85	3.99	CγH$_3$ 1.28	Lys36	9.19	4.18	1.72	CγH$_2$ 1.60, C$^\delta$H$_2$ 1.75, C$^\epsilon$H$_2$ 3.05
Tyr8	9.37	5.38	3.42, 2.95	C$^\delta$H$_2$ 7.28, C$^\epsilon$H$_2$ 7.13	Gln37	7.57	4.11	2.30, 2.26	CγH 2.47, 2.50, N$^\epsilon$H$_2$ 7.89, 6.95
					Thr38	8.25	4.33	3.37	C$^\delta$H$_2$ 7.01, C$^\epsilon$H$_2$ 6.73
Lys9	9.15	5.29	2.02, 1.99	CγH 1.50, 1.41, C$^\delta$H$_2$ 1.64, C$^\epsilon$H$_2$ 2.85, 2.88	Ala39	9.24	3.84	1.87	
					Asn40	8.48	4.53	2.98, 3.00	N$^\delta$H 7.79, 7.14
					Asp41	8.83	4.21	2.83, 2.71	
Leu10	8.70	5.05	0.95	C$_\gamma$H$_2$ 0.93, C$^\delta$H$_3$ 1.05	Asn42	7.43	4.72	2.77, 2.11	N$^\delta$H 6.75, 6.56
					Gly43	7.78	3.98		
Val11	9.21	4.31	2.00	CγH$_3$ 0.88	Val44	8.24	4.12	1.88	CγH$_3$ 0.83, 0.73
Ile12	8.74	4.30	1.65	CγH$_2$ 1.41, CγH$_3$ 0.76, C$^\delta$H$_3$ 0.69	Asp45	8.57	5.00	2.82, 2.71	
					Gly46	8.21	4.21, 3.87		
Asn13	8.96	5.23	2.95, 2.60	N$^\delta$H 7.21, 6.85	Glu47	8.15	4.84	2.16, 2.05	CγH 2.41, 2.48
Gly14	7.88	4.35, 4.11			Trp48	9.39	5.37	3.34, 3.22	C$^{\delta1}$H 7.60, C$^{\epsilon3}$H 7.60, Cζ^3H 6.65, N$^\epsilon$H 10.55, Cζ^2H 7.33, C$^{\eta2}$H 6.77
Lys15	8.85	4.17	1.88	CγH$_2$ 1.51, C$^\delta$H$_2$ 1.76, C$^\epsilon$H$_2$ 3.03					
					Thr49	9.33	4.88	4.31	CγH$_3$ 1.26
Thr16	8.65	4.41	4.22	CγH$_3$ 1.20	Tyr50	8.66	5.05	2.93, 2.60	C$^\delta$H 7.79, C$^\epsilon$H 7.14
Leu17	7.93	4.32	1.71	CγH$_2$ 1.43, C$^\delta$H$_3$ 0.93, 0.86	Asp51	7.61	4.64	2.69, 2.34	
					Asp52	8.62	4.17	2.88, 2.60	
Lys18	8.06	4.85	1.86, 1.79	CγH$_2$ 1.53, C$^\delta$H$_2$ 1.79, C$^\epsilon$H$_2$ 3.04	Ala53	8.34	4.17	1.55	
					Thr54	7.02	4.43		
Gly19	8.30	4.26, 4.21			Lys55	7.88	4.24	2.08	CγH$_2$ 1.91
Glu20	8.40	5.68	2.07, 2.02	CγH 2.35, 2.31	Thr56	7.42	5.50	3.79	CγH$_3$ 1.01
Thr21	8.81	4.78	4.02	CγH$_3$ 0.63	Phe57	10.45	5.69	3.34, 3.23	C$^\delta$H$_2$ 7.79, C$^\epsilon$H$_2$ 7.79, CζH 7.79
Thr22	8.18	5.91	4.40	CγH$_3$ 1.25	Thr58	9.19	5.31	3.85	CγH$_3$ 0.98
Thr23	9.10	4.71	3.91	CγH$_3$ 0.52	Val59	8.54	4.55	0.05	CγH$_3$ 0.36, −0.42
Glu24	8.08	5.50	1.79, 2.05	CγH 2.41, 2.35	Thr60	8.48	4.77	3.93	CγH$_3$ 1.24
Ala25	9.39	5.03	1.43		Glu61	8.29	4.54	2.21, 2.09	CγH 2.40, 2.48
Val26	8.70	4.43	2.28	CγH$_3$ 1.05	Lys62	8.73	4.63	1.90, 1.89	CγH$_2$ 1.57, C$^\delta$H$_2$ 1.76, C$^\epsilon$H$_2$ 3.04
Asp27	7.41	4.82	3.08		Pro63		4.46	2.32, 2.00	CγH 2.11, C$^\delta$H 3.95, 3.75
Ala28	8.45	3.37	1.23		Glu64	7.99	4.22	2.14, 1.96	CγH 2.41, 2.38

[a] Chemical shifts are reported with respect to sodium 2,2-dimethyl-2-silapentane-5-sulfonate. [b] Signals from this residue were not detected.

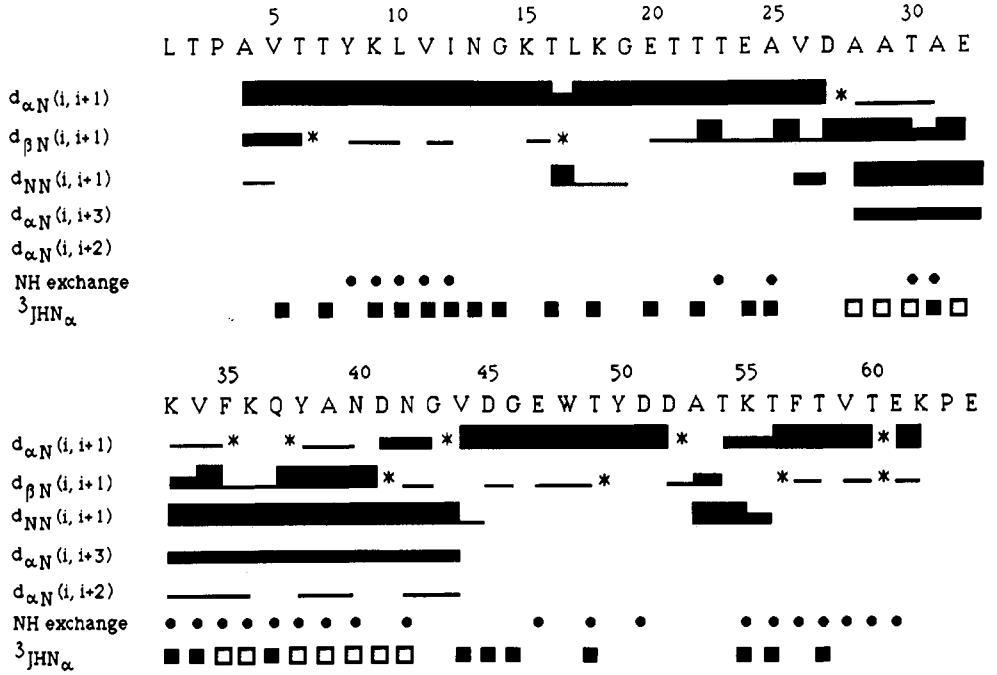

FIGURE 3: Summary of all short-range NOEs involving NH, C$^\alpha$H, and C$^\beta$H protons, the $^3J_{NH\alpha}$ coupling constants, and slowly exchanging amide protons. The relative strengths of the NOEs are classified into strong, medium, and weak, as indicated by the thickness of the lines. Potential connectivities that are obscured by overlaps are indicated by asterisks. The circles (●) indicate amide protons that did not exchange with D_2O after 12 h at 25 °C. Coupling constant data is summarized as follows: $^3J_{NH\alpha} > 8$ Hz (■); $^3J_{NH\alpha} < 6$ Hz (□).

the experimental conditions used here, the side-chain amino protons undergo intermediate exchange with water, thereby broadening their NH_3^+ resonances.

The sequence-specific resonance assignment was achieved from the NOESY spectrum by standard procedures. The starting point for the sequential assignment was Trp48, the

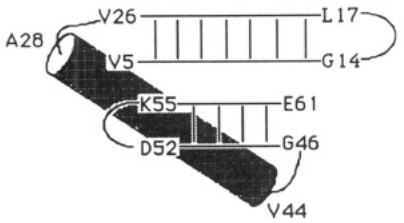

FIGURE 4: Schematic illustration of the arrangement of secondary structure in the IgG-binding domain of protein G.

only Trp residue in the amino acid sequence. The total spin system of this residue was identified from a combination of the TOCSY and NOESY experiments. The assignments were based on the interresidue sequential NOE connectivities, $d_{\alpha N(i,i+1)}$, $d_{\beta N(i,i+1)}$, and $d_{NN(i,i+1)}$ (Figure 2). Sequence-specific assignment of Pro63 was based on the NOE connectivities between Pro$^{\delta}$CH and C$^{\alpha}$H ($i - 1$). The presence of these cross-peaks also indicates that the X($i - 1$)–Pro(i) peptide bond is in the trans conformation. Assignment of the resonances from Pro3 was made by elimination. A complete list of the assignments is given in Table I.

Secondary Structure Elements in the IgG-Binding Domain of Protein G. A summary of the short-range NOEs involving NH, C$^{\alpha}$H, and C$^{\beta}$H is given in Figure 3. Regular secondary structure elements are usually identified from a qualitative interpretation of NOEs, C$^{\alpha}$H–NH coupling constants, and amide proton exchange rates (Wagner, 1990); information on coupling constants and NH exchange is included in Figure 3. Extended stretches of $d_{\alpha N(i,i+1)}$ connectivities, accompanied by large values (>8 Hz) for the $^3J_{HN\alpha}$ coupling constants, are indicative of extended β strands in the protein structure. The presence of an α-helix is demonstrated by a significant stretch of $d_{NN(i,i+1)}$ NOEs together with corresponding small values (<6 Hz) of $^3J_{HN\alpha}$. Estimated values of the $^3J_{HN\alpha}$ coupling constants of >8 and <6Hz were interpreted in terms of the ϕ torsion angles of $-160° < \phi < -80°$ and $-90° < \phi < 40°$ respectively (Pardi et al., 1984).

An α-helical region involving residues Ala28–Val44 can be deduced on the basis of the pattern of short-range $d_{NN(i,i+1)}$ being stronger than $d_{\alpha N(i,i+1)}$ and the prevalence of small (<6 Hz) $^3J_{HN\alpha}$ coupling constants. In addition, continuous $d_{\alpha N(i,i+3)}$ and a number of $d_{\alpha N(i,i+2)}$ and $d_{\alpha N(i,i+4)}$ NOEs are also observed in this region of the polypeptide chain.

Two regions of antiparallel β-sheet structure have been identified comprising residues Val5–Val26 and Asp45–Thr62. The antiparallel β-sheet from residues Val5 to Val26 was deduced on the basis of the pattern of short-range $d_{\alpha N(i,i+1)}$ and $d_{NN(i,i+1)}$, as well as long-range cross-strand $d_{\alpha\alpha(i,j)}$, $d_{\alpha N(i,j)}$ and $d_{NN(i,j)}$ NOEs, the occurrence of large $^3J_{HN\alpha}$ (>8 Hz) coupling constants, and some long-range side chain to side chain NOEs between residues on each of the two adjacent strands of the sheet. A turn involving residues Lys15, Thr16, and Leu17 can be deduced from the NOE pattern around this region of the polypeptide chain. A strong $d_{NN(i,i+1)}$ NOE between Thr16 and Leu17 together with a strong $d_{\alpha N(i,i+1)}$ NOE between Lys15 and Thr16 suggests a type II turn. The distribution of the slowly exchanging backbone amide protons can be explained on the basis of hydrogen bonding between the two strands. However, the exchange characteristics of the amide protons at either end of the strand did not conform with this hydrogen-bonding pattern; this is probably due to distortion of the regular β-sheet at each end. This is supported by the absence at the ends of the β-sheet of the interstrand NOEs that would be anticipated for a regular β-sheet.

A second β-sheet was identified involving the segments Asp45–Asp51 and Thr56–Lys62. This is also an antiparallel β-sheet with an interconnecting segment containing a type I turn involving residues Ala53, Thr54, and Lys55. This was deduced from the NOE pattern; strong $d_{NN(i,i+1)}$ NOEs are observed from Ala53 to Thr54 and from Thr54 to Lys55. The amide proton exchange characteristics also indicate hydrogen-bonding patterns typical of a regular β-sheet with distortion at the ends. This structure is supported by the interstrand NOE patterns. In addition, long-range $d_{\alpha\alpha(i,j)}$, $d_{\alpha N(i,j)}$, and $d_{NN(i,j)}$ NOEs were observed between the residues in the segments Lys9–Gly14 and Thr56–Glu61. This pattern of NOEs suggests that the two segments are packed together in a manner that resembles a parallel β-sheet. A schematic representation of the secondary structure of the IgG-binding domain of protein G is shown in Figure 4. We would anticipate a similar organization of secondary structure in the other two IgG-binding domains in protein G on the basis of the high degree of sequence homology with the protein studied here. The structure is clearly different from that of the IgG-binding domain from protein A, which consists of three consecutive α-helices (Torigoe et al., 1990). It appears, therefore, that two proteins of quite different structure have evolved to bind to the same site on the Fc portion of IgG. A more detailed comparison must await the calculation of the three-dimensional structure of the protein G domain, which is in progress.

ACKNOWLEDGMENTS

We are indebted to Drs. K. Lilley and L. Packman for the molecular mass measurements.

REFERENCES

Basus, V. J. (1989) *Methods in Enzymology* (Oppenheimer, N. J., & James, T. L., Eds.) pp 132–149, Academic Press, London.

Bax, A., & Davis, D. G. (1985) *J. Magn. Reson. 65*, 355–360.

Björck, L., & Åkerström, B. (1990) in *Bacterial Immunoglobulin-Binding Proteins* (Boyle, M. D. P., Ed.) pp 113–126, Academic Press, New York.

Deisenhofer, J. (1981) *Biochemistry 20*, 2361–2370.

Fahnestock, S. R., Alexander, P., Filpula, D., & Nagle, J. (1990) in *Bacterial Immunoglobulin-Binding Proteins* (Boyle, M. D. P., Ed.) pp 133–148, Academic Press, New York.

Goward, C. R., Murphy, J. P., Atkinson, T., & Barstow, D. A. (1990) *Biochem. J. 267*, 171–177.

Goward, C. R., Irons, L. I., Murphy, J. P., & Atkinson, T. (1991) *Biochem. J. 274*, 501–507.

Guss, B., Eliasson, M., Olsson, A., Uhlén, M., Frej, A.-K., Jörnvall, H., Flock, J.-I., & Lindberg, M. (1986) *EMBO J. 5*, 1567–1575.

Langone, J. J. (1982) *Adv. Immunol. 32*, 158–252.

Lian, L. Y. (1988) *Biochem. Biophys. Res. Commun. 154*, 1253–1259.

Marion, D., & Bax, A. (1988) *J. Magn. Reson. 79*, 352–356.

Marion, D., & Wüthrich, K. (1983) *Biochem. Biophys. Res. Commun. 113*, 967–974.

Olsson, A., Eliasson, M., Guss, B., Nilsson, B., Hellman, U., Lindberg, M., & Uhlén, M. (1987) *Eur. J. Biochem. 168*, 319–324.

Pardi, A., Billeter, M., & Wüthrich, K. (1984) *J. Mol. Biol. 180*, 741–751.

Redfield, A., & Kuntz, S. D. (1975) *J. Magn. Reson. 19*, 250–254.

Shaka, A. J., Lee, C. J., & Pines, A. (1988) *J. Magn. Reson. 77*, 274–293.

Skelenar, V., & Bax, A. (1987) *J. Magn. Reson. 74*, 469–479.

Stone, G. C., Sjöbring, U., Björck, L., Sjöquist, J., Barber, C. V., & Nardella, F. A. (1989) *J. Immunol. 143*, 565–570.
Torigoe, H., Shimada, I., Saito, A., Sato, M., & Arata, Y. (1990) *Biochemistry 29*, 8787–8793.
Wagner, G. (1990) *Prog. Nucl. Magn. Reson. Spectrosc. 22*, 101–139.
Wüthrich, K. (1986) *NMR of Proteins and Nucleic Acids*, Wiley, New York.

Articles

Full Replacement of the Function of the Secondary Electron Acceptor Phylloquinone(=Vitamin K_1) by Non-Quinone Carbonyl Compounds in Green Plant Photosystem I Photosynthetic Reaction Centers†

Shigeru Itoh* and Masayo Iwaki

Division of Bioenergetics, National Institute for Basic Biology, 38 Nishigonaka, Myodaiji, Okazaki 444, Japan
Received November 14, 1990; Revised Manuscript Received March 6, 1991

ABSTRACT: One-carbonyl quinonoid compounds, fluorenone (fluoren-9-one), anthrone, and their derivatives are introduced into spinach photosystem (PS) I reaction centers in place of the intrinsic secondary electron acceptor phylloquinone (=vitamin K_1). Anthrone and 2-nitrofluorenone fully mediated the electron-transfer reaction between the reduced primary electron acceptor chlorophyll A_0^- and the tertiary electron acceptor iron–sulfur centers. It is concluded that the PS I phylloquinone-binding site has a structure that enables various compounds with different molecular structures to function as the secondary acceptor and that the reactions of incorporated compounds are mainly determined by their redox properties rather than by their molecular structure. Carbonyl groups increase the binding affinity of the quinone/quinonoid compounds but do not seem to be essential to their function. The quinonoid compounds as well as quinones incorporated into the PS I phylloquinone-binding sites are estimated to function at redox potentials more negative than in organic solvents.

In the photosystem I reaction center (PS I RC)[1] of green plants, absorption of light oxidizes the special RC chlorophyll P700 and initiates a series of electron-transfer steps as shown in Figure 1 [see reviews by Andréasson and Vängard (1988), Golbeck (1987), and Mathis (1990)]. The primary electron acceptor A_0 is chlorophyll *a*-690 (Shuvalov et al., 1986; Wasielewski et al., 1987; Mathis et al., 1988), and A_1 is the secondary electron acceptor phylloquinone (2-methyl-3-phytyl-1,4-naphthoquinone = vitamin K_1); F_X, F_A, and F_B represents iron–sulfur center X, A, or B (Golbeck, 1987). These cofactors, except F_A/F_B on a 9-kDa small subunit polypeptide, reside on the RC complex made of two 80-kDa molecular polypeptides (Kirsch et al., 1986; Golbeck, 1987).

We developed an extraction/reconstitution method of phylloquinone in spinach PS I particles and provided the direct evidence for the chemical identity of A_1 (Itoh et al., 1987; Itoh & Iwaki, 1988) as confirmed in cyanobacterial membranes (Biggins & Mathis, 1988; Ikegami & Katoh, 1989). One of two phylloquinone molecules contained in the PS I RC complex (Takahashi et al., 1985; Schoeder & Lockau, 1986; Malkin, 1986) is now estimated to function as A_1 (Brettel et al., 1986; Itoh et al., 1987; Ikegami et al., 1987; Biggins & Mathis, 1988; Itoh & Iwaki 1989a), although some arguments still remain (Warden, 1990). The extraction of phylloquinone stops the oxidation of A_0^- and enhances the charge recombination reaction between A_0^- and $P700^+$ (Itoh et al., 1987; Ikegami et al., 1987; Biggins & Mathis, 1988; Itoh & Iwaki, 1989a). This reaction produces a triplet state of P700 ($P700^T$) (Ikegami et al., 1987) or delayed fluorescence (Itoh & Iwaki, 1988) and depresses the $P700^+$ amount detectable in the microsecond–millisecond time range after flash excitation. Reconstitution of phylloquinone (Itoh et al., 1987; Itoh & Iwaki, 1988, 1989a; Biggins & Mathis, 1988) or other quinones (Iwaki & Itoh, 1989, 1990, 1991a; Kim et al., 1989; Biggins, 1990) recovers the rapid oxidation of A_0^- by the quinone and stabilizes $P700^+$ until the microsecond–millisecond time range. The phylloquinone-binding site accepts various benzo-, naphtho-, and anthraquinones (Iwaki & Itoh, 1989, 1990, 1991a,b) as well as quinone site inhibitors (Itoh & Iwaki, 1989b, 1990). We thus proposed to call this electron acceptor phylloquinone (A_1) as Q_ϕ and its binding site as the Q_ϕ site to facilitate comparison with the other quinone functional sites in photosynthetic or respiratory electron-transfer systems (Itoh & Iwaki, 1989b).

† This work is supported by grants-in-aid for Cooperative Research and for Scientific Research from the Japanese Ministry of Education, Science, and Culture to S.I.
* Address correspondence to this author.

[1] Abbreviations: PS, photosystem, RC, reaction center; A_0 and A_1, PS I primary and secondary (=phylloquinone) electron acceptors, respectively; AN, acetonitrile; DMF, dimethylformamide; E_m, redox midpoint potential; $E_{1/2}$, polarographically measured half-wave redox potential; F_X, F_A, and F_B, iron–sulfur centers X, A, and B; P700, photosystem I primary electron donor chlorophyll *a*; Q_A and Q_B, secondary and tertiary electron acceptor quinones in photosystem II or purple bacterial RF; Q_ϕ, quinones functioning as A_1 (including phylloquinone); $t_{1/2}$, half decay time.

0006-2960/91/0430-5340$02.50/0 © 1991 American Chemical Society